

# Deterministic Hallucination Detection in Medical VQA via Confidence-Evidence Bayesian Gain

Mohammad Asadi<sup>1</sup>, Tahoura Nedae<sup>2</sup>, Jack W. O’Sullivan<sup>3,4</sup>, Euan Ashley<sup>3,4</sup>,  
and Ehsan Adeli<sup>4,5,6</sup>

<sup>1</sup> Department of Electrical Engineering, Stanford University, CA, USA  
Department of Biology, Stanford University, CA, USA

<sup>2</sup> Division of Cardiology, Department of Medicine, Stanford University, CA, USA

<sup>3</sup> Department of Biomedical Data Science, Stanford University, CA, USA

<sup>4</sup> Department of Computer Science, Stanford University, CA, USA

<sup>5</sup> Department of Psychiatry and Behavioral Sciences, Stanford University, CA, USA

**Abstract.** Multimodal large language models (MLLMs) have shown strong potential for medical Visual Question Answering (VQA), yet they remain prone to hallucinations, defined as generating responses that contradict the input image, posing serious risks in clinical settings. Current hallucination detection methods, such as Semantic Entropy (SE) and Vision-Amplified Semantic Entropy (VASE), require 10 to 20 stochastic generations per sample together with an external natural language inference model for semantic clustering, making them computationally expensive and difficult to deploy in practice. We observe that hallucinated responses exhibit a distinctive signature directly in the model’s own log-probabilities: inconsistent token-level confidence and weak sensitivity to visual evidence. Based on this observation, we propose **Confidence-Evidence Bayesian Gain (CEBaG)**, a deterministic hallucination detection method that requires no stochastic sampling, no external models, and no task-specific hyperparameters. CEBaG combines two complementary signals: *token-level predictive variance*, which captures inconsistent confidence across response tokens, and *evidence magnitude*, which measures how much the image shifts per-token predictions relative to text-only inference. Evaluated across four medical MLLMs and three VQA benchmarks (16 experimental settings), CEBaG achieves the highest AUC in 13 of 16 settings and improves over VASE by 8 AUC points on average, while being fully deterministic and self-contained. The code will be made available upon acceptance.

**Keywords:** Hallucination detection · Medical VQA · Multimodal LLMs.

## 1 Introduction

Medical Visual Question Answering (VQA), powered by multimodal large language models (MLLMs), enables the interpretation of medical images in response to natural language queries, supporting tasks from abnormality detection to differential diagnosis [28, 20]. However, MLLMs are susceptible to *hallucinations*,

defined as responses that misinterpret or contradict the input image, posing substantial risks including misdiagnoses, inappropriate treatments, and diminished clinician trust [9, 21]. Despite efforts in data optimization [30], training [10], and decoding refinements [27], hallucinations remain a persistent challenge, highlighting the need for effective detection methods.

Recent approaches to hallucination detection include detector fine-tuning [6], cross-checking [30, 3], external fact retrieval [22], visual evidence verification [29], and uncertainty estimation [17, 1, 4, 31]. Among these, uncertainty estimation stands out for its simplicity, as it uses only the model itself without additional annotated data or external knowledge bases [9, 21]. Semantic Entropy (SE) [4] quantifies uncertainty by computing entropy over semantically clustered responses. Vision-Amplified Semantic Entropy (VASE) [18] extends SE by contrasting semantic distributions from original and augmented images, amplifying the influence of visual input. Other contrastive methods such as VCD [13] and LCD [14] leverage output differences under perturbed inputs, while Semantic Entropy Probes [12] train a probe on internal activations, requiring task-specific data unlike our training-free approach. A common thread in all these methods is their reliance on stochastic sampling, external models, or additional training, which raises the question of whether the uncertainty signal they seek is already accessible through simpler means.

These methods also face a concrete efficiency bottleneck. SE requires  $M$  stochastic generations (typically  $M=10$ ) with high-temperature sampling, followed by pairwise semantic equivalence checks via an external NLI model [7]. VASE doubles this to  $2M$  generations plus  $O(M^2)$  NLI comparisons per input, making it prohibitive for clinical deployment where real-time feedback is essential. We propose **Confidence-Evidence Bayesian Gain (CEBaG)**, which replaces stochastic sampling with deterministic log-probability analysis. CEBaG combines two complementary signals: *token-level predictive variance* (the standard deviation of per-token log-probabilities, elevated when the model fabricates content) and *evidence magnitude* (the absolute per-token log-probability shift when the image is present versus absent, capturing the strength of visual grounding). The resulting score,  $\sigma \cdot (1 + |G|/L)$ , is parameter-free, requires only one generation and two scoring passes, uses no external models, and is fully deterministic (Fig. 1).

Our contributions are: (1) We propose CEBaG, a deterministic hallucination detection method requiring three forward passes and no external models, compared to 20+ stochastic generations and an NLI model for SE/VASE. (2) We conduct an extensive evaluation spanning four MLLMs (MedGemma-4b, MedGemma-1.5-4b, HuatuoGPT-Vision-7B, LLaVA-Med-v1.5-7B) and three datasets (VQA-RAD, SLAKE, PathVQA), 16 settings in total. (3) CEBaG consistently outperforms SE, VASE, and RadFlag [26], achieving the best AUC in 13 of 16 settings and improving over VASE by 8 AUC points on average.

## 2 Method

Given a medical image  $x_v$ , a textual question  $x_q$ , and a medical MLLM  $f$ , the model generates a response  $r = f(x_v, x_q)$  via greedy or low-temperature decoding. Our goal is to determine whether  $r$  is a hallucination (a response that contradicts the visual evidence in  $x_v$ ) without access to ground-truth answers. For evaluation, we follow prior work [18, 4] and use the GREEN model [23] to produce reference-based ground-truth labels.

### 2.1 Evidence Gain as Pointwise Mutual Information

The key quantity in CEBaG is the *evidence gain*: how much the model’s belief in its own answer changes when it observes the image. Formally, we interpret the text-only probability  $P(r | x_q)$  as the model’s **language prior**, i.e., its belief about the answer based solely on the question and its pre-trained knowledge. The multimodal probability  $P(r | x_v, x_q)$  represents the **posterior** belief after updating with the visual evidence  $x_v$ . We use “prior” and “posterior” in the information-theoretic sense:  $P(r | x_q)$  represents the model’s belief before observing visual evidence, and  $P(r | x_v, x_q)$  its updated belief after conditioning on the image. This is distinct from Bayesian inference over model parameters; rather,  $G$  captures how the image updates the model’s predictive distribution for a fixed set of parameters. The sequence log-probabilities are defined as:

$$\log P(r | x_v, x_q) = \sum_{j=1}^L \log P(r_j | r_{<j}, x_v, x_q), \quad (1)$$

$$\log P(r | x_q) = \sum_{j=1}^L \log P(r_j | r_{<j}, x_q). \quad (2)$$

The **evidence gain**  $G$  is defined as the difference between the posterior and the prior:

$$G = \log P(r | x_v, x_q) - \log P(r | x_q). \quad (3)$$

By Bayes’ rule,  $P(r | x_v, x_q) = \frac{P(x_v | r, x_q)P(r | x_q)}{P(x_v | x_q)}$ . Substituting this into Eq. (3):

$$G = \log \left( \frac{P(x_v | r, x_q)P(r | x_q)}{P(x_v | x_q)} \right) - \log P(r | x_q) = \log P(x_v | r, x_q) - \log P(x_v | x_q). \quad (4)$$

Since  $\log P(x_v | x_q)$  is constant with respect to the response  $r$ ,  $G$  is directly proportional to  $\log P(x_v | r, x_q)$ , the log-likelihood of the image given the response. Thus,  $G$  can be seen as the **Pointwise Mutual Information (PMI)** between the response and the image (conditioned on the question). A large positive  $G$  implies that the response makes the observed image highly probable (strong grounding), while a negative  $G$  suggests the response contradicts the visual evidence.

To obtain a length-normalized measure of visual influence, we define the **evidence magnitude**:

$$E = \frac{|G|}{L}, \quad (5)$$

which captures the average absolute shift in belief per token. We use the magnitude  $|G|$  because a strong visual influence (increasing or decreasing token probabilities) indicates attention to the image, whereas a lack of influence ( $G \approx 0$ ) suggests the model is relying entirely on its language prior.

## 2.2 Confidence-Evidence Bayesian Gain

We propose CEBaG, a scoring function that combines the model’s internal uncertainty with its sensitivity to visual evidence. We define the **token-level predictive variance**:  $\sigma = \text{std}_{j=1}^L[\log P(r_j | r_{<j}, x_v, x_q)]$ , which measures the consistency of the model’s confidence across the generated sequence. High  $\sigma$  indicates “confidence spikes” on function words interspersed with low-confidence content tokens, a pattern characteristic of hallucination. The CEBaG score is defined as:

$$\text{CEBaG} = \sigma \cdot (1 + E). \quad (6)$$

This formulation can be interpreted as **posterior uncertainty weighted by visual information gain**. Hallucinations typically arise in two scenarios: (1) The model is uncertain about the content ( $\sigma$  is high); or (2) The visual evidence causes a large shift in belief ( $E$  is high) but fails to resolve the uncertainty (or contradicts the language prior).

The multiplicative term  $(1 + E)$  amplifies the base uncertainty  $\sigma$  when the response is highly sensitive to the image, flagging cases where the model is “struggling” to reconcile visual evidence with its language prior. Importantly, this formulation is **hyperparameter-free**, requiring no hyperparameter tuning or normalization, making it robust across different models and datasets. Unlike SE and VASE, which require configuring the number of generations  $M$ , sampling temperature  $T$ , and (for VASE) the amplification ratio  $\alpha$ , CEBaG applies the same fixed formula across all models and datasets.

## 3 Experiments

**Datasets:** We evaluate on three medical VQA benchmarks: *VQA-RAD* [15] (451 test samples, including 200 open-ended), a radiology VQA dataset covering chest X-rays, CT, and MRI; *SLAKE* [19], a bilingual medical VQA dataset with semantically labeled knowledge (1061 test samples); and *PathVQA* [8] (1000 test samples), covering pathology images. For VQA-RAD, we report performance on both open-ended questions and all questions (including yes/no), following [18].

**Models:** We evaluate four medical MLLMs spanning two architecture families: *MedGemma-4b-it* and *MedGemma-1.5-4b-it* [25] (encoder-decoder), and *HuatuoGPT-Vision-7B* [2] and *LLaVA-Med-v1.5-Mistral-7B* [16] (LLaVA-style decoder-only).

**Ground truth and metrics:** Following the evaluation protocol established by VASE [18], we use the GREEN model [23] to generate reference-based ground-truth labels: a response is labeled as hallucinated if its GREEN score falls below

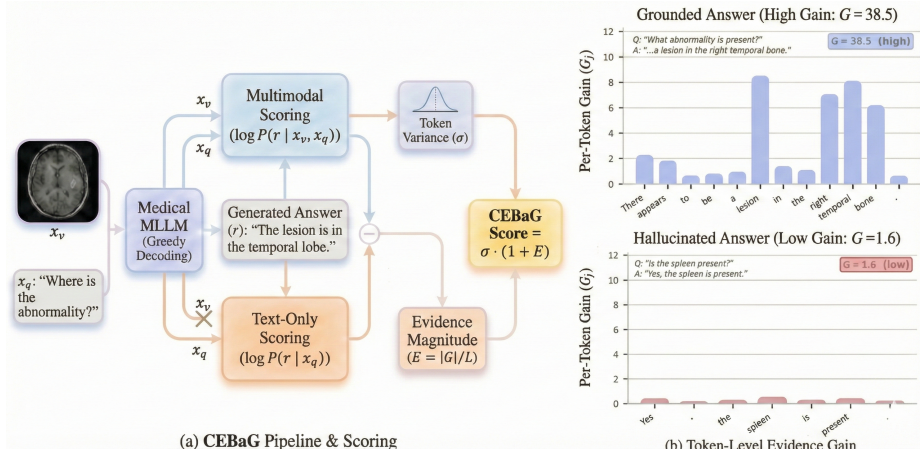


**Fig. 1.** Overview of CEBaG for hallucination detection in medical VQA. (a) The CEBaG pipeline on a concrete example: the model generates answer  $r$ , which is scored under two conditions, with and without the image, yielding two signals: token-level predictive variance  $\sigma$  and evidence magnitude  $E=|G|/L$ . CEBaG combines these as  $\sigma \cdot (1+E)$ . (b) Per-token evidence gain for a **grounded** answer (top;  $G=38.5$ , image strongly increases confidence on clinical tokens like “lesion” and “temporal”) versus a **hallucinated** answer (bottom;  $G=1.6$ , image barely changes confidence). Both charts share the same  $y$ -axis scale, making the contrast immediately visible.

1.0. We adopt this protocol to ensure direct comparability with prior work and use the same metrics (AUC and AUG) as [18].

**Baselines.** We compare CEBaG against four state-of-the-art hallucination detection methods: (1) *AvgProb* [11], which uses the average token probability in the sequence; (2) *Semantic Entropy (SE)* [4], which measures uncertainty over semantic clusters of generated answers; (3) *Vision-Amplified Semantic Entropy (VASE)* [18], which enhances SE by generating additional answers conditioned on visually augmented images; and (4) *RadFlag* [26], which checks for consistency between the generated answer and the findings in the radiology report. We adhere to the official implementations and hyperparameters for all baselines. For SE and VASE, we use 10 generations (plus 10 augmented for VASE) and a temperature of 1.0, as specified in their respective papers.

**Implementation details.** For CEBaG, the generated answer  $r$  is produced via greedy decoding (temperature  $T=0.1$ ). The two scoring passes (Eqs. 1–2) use teacher-forced forward passes;  $\sigma$  is computed from the same forward pass as  $\log P(r | x_v, x_q)$  at no additional cost. For the text-only pass, visual input is removed at the interface level: for MedGemma, no image is included in the chat message and no pixel values are passed to the model; for LLaVA-style models (LLaVA-Med, HuatuoGPT), the `<image>` token is removed from the prompt template and the processor is called without image input. This ensures a clean text-only baseline across all architectures. All experiments were conducted on 8

**Table 1.** Hallucination detection performance: AUC (%) $\uparrow$  and AUG (%) $\uparrow$  across four medical LLMs and three VQA datasets. Best results per row are in **bold**; second best are underlined. CEBaG achieves the best AUC in 13 of 16 settings.

Dataset	AvgProb [11]		SE [4]		VASE [18]		RadFlag [26]		CEBaG (Ours)	
	AUC	AUG	AUC	AUG	AUC	AUG	AUC	AUG	AUC	AUG
<i>MedGemma-4b-it</i> [25]										
VQA-RAD (Open)	39.9	48.0	<b>61.9</b>	<b>65.3</b>	60.8	63.3	58.4	63.6	<u>61.0</u>	<u>64.8</u>
VQA-RAD (All)	42.9	54.6	52.2	58.0	<u>57.6</u>	<u>59.9</u>	54.7	58.9	<b>60.8</b>	<b>64.6</b>
SLAKE	35.3	52.9	54.9	64.2	<u>62.6</u>	<u>70.1</u>	57.0	66.2	<b>71.9</b>	<b>75.9</b>
PathVQA	46.4	45.1	58.0	48.9	<u>61.5</u>	<u>49.6</u>	56.8	47.4	<b>71.9</b>	<b>59.0</b>
<i>MedGemma-1.5-4b-it</i> [25]										
VQA-RAD (Open)	69.1	47.4	53.2	37.2	<u>60.1</u>	<u>40.3</u>	54.5	39.3	<b>72.9</b>	<b>47.2</b>
VQA-RAD (All)	63.6	56.2	53.4	48.6	<u>54.8</u>	<u>51.5</u>	54.3	46.3	<b>66.9</b>	<b>58.2</b>
SLAKE	57.4	52.0	<u>57.7</u>	51.9	<b>59.5</b>	<u>52.9</u>	57.2	<b>53.0</b>	57.5	52.0
PathVQA	65.9	48.9	56.8	40.9	<u>60.1</u>	<u>45.7</u>	56.3	41.6	<b>66.6</b>	<b>48.8</b>
<i>HuatuogPT-Vision-7B</i> [2]										
VQA-RAD (Open)	43.7	48.1	<u>64.1</u>	<u>62.8</u>	61.7	59.6	59.9	58.4	<b>70.4</b>	<b>63.1</b>
VQA-RAD (All)	39.3	52.2	58.3	65.1	58.9	<u>66.1</u>	<u>60.0</u>	63.5	<b>67.7</b>	<b>67.6</b>
SLAKE	30.5	38.4	57.7	54.9	59.9	<u>58.0</u>	<u>60.6</u>	54.2	<b>67.0</b>	<b>64.2</b>
PathVQA	30.5	28.7	53.6	38.2	53.2	<u>39.5</u>	<u>55.5</u>	38.9	<b>82.0</b>	<b>55.6</b>
<i>LLaVA-Med-v1.5-Mistral-7B</i> [16]										
VQA-RAD (Open)	62.9	38.6	63.8	<b>40.4</b>	<b>68.4</b>	<u>40.2</u>	<u>65.8</u>	40.1	65.8	39.1
VQA-RAD (All)	58.8	48.7	58.1	<b>50.7</b>	57.6	49.3	56.8	48.1	<b>62.1</b>	<u>50.0</u>
SLAKE	59.9	50.0	57.9	50.2	57.4	<u>50.8</u>	<u>58.7</u>	50.7	<b>63.8</b>	<b>52.3</b>
PathVQA	75.1	52.0	57.4	41.3	60.4	41.7	58.8	39.7	<b>77.6</b>	<b>53.1</b>
<b>Average</b>	51.3	47.6	57.4	51.2	59.6	52.4	57.8	50.6	<b>67.9</b>	<b>57.2</b>

NVIDIA H100 GPUs. Following the evaluation protocol of SE [4] and VASE [18], we report point estimates of AUC and AUG. We note that CEBaG is fully deterministic, eliminating the run-to-run variance inherent in sampling-based baselines; the reported scores are therefore exact for a given model’s generated answer.

### 3.1 Main Results

Table 1 presents the hallucination detection performance across all 16 experimental settings. CEBaG achieves the best AUC in **13 of 16** settings and ranks in the top two in 15 of 16. On average, CEBaG attains 67.9% AUC, outperforming VASE (59.6%), SE (57.4%), and RadFlag (57.8%) by substantial margins, with an improvement of +8.2 AUC points over the previous state-of-the-art VASE. Significantly, CEBaG achieves this without any hyperparameter tuning.

The gains are particularly pronounced on larger datasets: on PathVQA, CEBaG outperforms VASE by +10.5 (MedGemma), +6.5 (MedGemma-1.5), +28.8 (HuatuogPT), and +17.2 (LLaVA-Med) AUC points. On SLAKE, the improvements are similarly large, with CEBaG surpassing VASE by +9.3 (MedGemma) and +7.1 (HuatuogPT). On the smaller VQA-RAD datasets, the improvements

**Table 2.** Computational cost and performance comparison. CEBaG requires an order of magnitude fewer forward passes and no external models, while achieving the highest average AUC and AUG across all 16 settings.

Method	Forward passes	External model	Deterministic	Hyperparams	$\overline{AUC}$	$\overline{AUG}$
AvgProb [11]	1 gen.	None	Yes	None	51.3	47.6
SE [4]	$M$ gen. + NLI	DeBERTa-MNLI	No	$M, T$	57.4	51.2
VASE [18]	$2M$ gen. + NLI	DeBERTa-MNLI	No	$M, T, \alpha$	59.6	52.4
RadFlag [26]	$M$ gen. + NLI	DeBERTa-MNLI	No	$M, T$	57.8	50.6
<b>CEBaG (Ours)</b>	1 gen. + 2 evals	None	Yes	None	<b>67.9</b>	<b>57.2</b>

remain consistent across most models, with CEBaG achieving the best AUC in 6 of 8 VQA-RAD settings. Furthermore, our method maintained stable detection performance across GREEN thresholds between 0.4 and 0.8, confirming its insensitivity to specific ground-truth boundaries.

### 3.2 Efficiency Analysis

Table 2 compares the computational requirements and resulting average performance for each method. With the standard setting  $M=10$ , SE requires 10 autoregressive generations plus  $O(M^2)=O(100)$  pairwise entailment comparisons per sample. VASE doubles the generation cost to 20 passes plus the same entailment overhead. RadFlag also requires  $M$  generations and entailment checks. All three methods additionally require loading and running a DeBERTa-v2-xlarge-MNLI model alongside the target MLLM, and all involve hyperparameters ( $M$ , sampling temperature  $T$ , and for VASE, the vision-amplified ratio  $\alpha$ ).

In contrast, CEBaG requires exactly **three forward passes**: one autoregressive generation and two teacher-forced scoring passes (with and without the image). No external model is needed, and no hyperparameters require tuning. The scoring passes are substantially cheaper than generation because they process fixed token sequences without autoregressive decoding. Moreover, CEBaG is **deterministic**, whereas sampling-based methods introduce variance that requires averaging over multiple runs for stable estimates. Despite its simplicity and efficiency, CEBaG achieves the highest average AUC (67.9%) and AUG (57.2%) across all settings, significantly outperforming the computationally expensive baselines.

### 3.3 Ablation Study

To understand the contribution of each component in CEBaG, we compare four variants:  $\sigma$  **only**, using only the token-level predictive variance;  $E$  **only**, using only the evidence magnitude  $|G|/L$ ; **CEBaG**, the full parameter-free formula  $\sigma \cdot (1 + E)$ ; and **CEBaG** $_{\lambda}$ , a tuned variant that uses min-max normalization and sweeps a scalar weight  $\lambda$  over a wide range, representing the best performance achievable with hyperparameter optimization for each individual dataset.

**Table 3.** Ablation study: AUC (%) $\uparrow$  of CEBaG components.  $\sigma$  only uses token-level variance alone;  $E$  only uses absolute per-token gain alone; CEBaG combines both (parameter-free); CEBaG $_{\lambda}$  adds a tunable weight (upper bound).

Setting	AUC (%)				AUG (%)			
	$\sigma$	$E$	CEBaG	CEBaG $_{\lambda}$	$\sigma$	$E$	CEBaG	CEBaG $_{\lambda}$
<i>MedGemma-4b-it</i>								
SLAKE	71.1	51.6	<u>71.9</u>	<b>73.5</b>	<u>74.8</u>	64.9	<b>75.9</b>	74.6
PathVQA	67.8	63.4	<u>71.9</u>	<b>77.5</b>	<u>55.6</u>	57.0	<b>59.0</b>	61.7
<i>MedGemma-1.5-4b-it</i>								
VQA-RAD (Open)	68.2	63.9	<u>72.9</u>	<b>75.7</b>	44.7	40.8	<u>47.2</u>	<b>47.0</b>
PathVQA	57.9	<u>70.8</u>	66.6	<b>77.8</b>	42.6	<u>52.2</u>	48.8	<b>56.3</b>
<i>HuatuogPT-Vision-7B</i>								
PathVQA	<u>80.6</u>	67.3	<b>82.0</b>	82.5	<u>55.3</u>	48.3	<b>55.6</b>	55.5
VQA-RAD (All)	<u>68.0</u>	53.8	67.7	<b>68.6</b>	<b>67.5</b>	59.6	<u>67.6</u>	66.9
<i>LLaVA-Med-v1.5-Mistral-7B</i>								
VQA-RAD (All)	<u>62.9</u>	52.0	62.1	<b>66.2</b>	<u>50.8</u>	45.6	50.0	<b>54.0</b>
SLAKE	<u>65.2</u>	51.8	63.8	<b>68.8</b>	<u>52.7</u>	46.8	52.3	<b>55.3</b>
<b>Average (all 16)</b>	67.0	59.0	<u>67.9</u>	<b>71.9</b>	53.8	50.5	<u>57.2</u>	<b>58.8</b>

Table 3 shows results on eight representative settings, with full averages across all 16 settings in the bottom row. Several patterns emerge: 1- Token-level variance is the dominant signal.  $\sigma$  only already achieves 67.0% average AUC, substantially outperforming all baselines (SE 57.4%, VASE 59.6%, RadFlag 57.8%), confirming that per-token log-probability variance is a powerful hallucination indicator on its own. 2- Evidence magnitude provides complementary information. While  $E$  only (59.0%) is weaker than  $\sigma$  only, the multiplicative combination in CEBaG (67.9%) outperforms  $\sigma$  only in 10 of 16 settings, with the largest gains on MedGemma-1.5 VQA-RAD Open (+4.7) and MedGemma PathVQA (+4.1). 3- The parameter-free formula is competitive with tuned variants. CEBaG $_{\lambda}$  (which sweeps over hyperparameter values for each specific model-dataset pair and selects the best, presenting the maximum achievable performance in that experimental setting) achieves 71.9% average AUC, only 4.0 points above CEBaG, demonstrating that the fixed formula  $\sigma \cdot (1 + E)$  captures nearly all available signal without dataset-specific tuning.

## 4 Conclusion

We introduced CEBaG, a deterministic hallucination detection method for medical VQA that combines token-level predictive variance and evidence magnitude into a unified score. Unlike sampling-based approaches (SE, VASE), which require 10–20 stochastic generations and an external NLI model, CEBaG relies on only three forward passes of the target model. Across four medical MLLMs and 16 experimental settings, CEBaG achieves the best AUC in 13 settings and surpasses state-of-the-art VASE by an average of 8 AUC points, while substantially

reducing computational cost. Its efficiency, simplicity, and zero-configuration design make it practical for real-time clinical deployment. A limitation is its reliance on access to model log-probabilities, restricting use to white-box models. Future work can extend CEBaG to black-box settings via output perturbation and explore applications in report generation and multi-turn clinical dialogue.

## 5 Acknowledgment

This work was partially supported by the NIH Grants AG089169, AG084471, Stanford HAI Hoffman-Yee Award & GCP Credits, and UST. Mohammad Asadi is supported by the Amazon AI PhD Fellowship and the Stanford HAI Graduate Fellowship.

## References

1. Chen, C., Liu, K., Chen, Z., Gu, Y., Wu, Y., Tao, M., Fu, Z., Ye, J.: INSIDE: LLMs’ internal states retain the power of hallucination detection. In: ICLR (2024)
2. Chen, J., Guo, D., Li, M., Lin, R., Shan, C., Zhao, Y., Shen, T., Wan, X.: HuatuoGPT-Vision, towards injecting medical visual knowledge into multimodal LLMs at scale. arXiv:2406.19280 (2024)
3. Cohen, R., Hamri, M., Geva, M., Globerson, A.: LM vs LM: Detecting factual errors via cross examination. In: EMNLP. pp. 12621–12640 (2023)
4. Farquhar, S., Kossen, J., Kuhn, L., Gal, Y.: Detecting hallucinations in large language models using semantic entropy. *Nature* **630**(8017), 625–630 (2024)
5. Favero, A., Zancato, L., Trager, M., Choudhary, S., Perera, P., Achille, A., Swaminathan, A., Soatto, S.: Multi-modal hallucination control by visual information grounding. In: CVPR. pp. 14303–14312 (2024)
6. Gunjal, A., Yin, J., Bas, E.: Detecting and preventing hallucinations in large vision language models. In: AAAI. vol. 38, pp. 18135–18143 (2024)
7. He, P., Liu, X., Gao, J., Chen, W.: DeBERTa: Decoding-enhanced BERT with disentangled attention. In: ICLR (2020)
8. He, X., Zhang, Y., Mou, L., Xing, E., Xie, P.: PathVQA: 30000+ questions for medical visual question answering. arXiv:2003.10286 (2020)
9. Huang, L., Yu, W., Ma, W., Zhong, W., Feng, Z., Wang, H., Chen, Q., Peng, W., Feng, X., Qin, B., et al.: A survey on hallucination in large language models: Principles, taxonomy, challenges, and open questions. *ACM Trans. Inf. Syst.* (2023)
10. Jiang, C., Xu, H., Dong, M., Chen, J., Ye, W., Yan, M., Ye, Q., Zhang, J., Huang, F., Zhang, S.: Hallucination augmented contrastive learning for multimodal large language model. In: CVPR. pp. 27036–27046 (2024)
11. Kadavath, S., Conerly, T., Askell, A., Henighan, T., Drain, D., Perez, E., Schiefer, N., Hatfield-Dodds, Z., DasSarma, N., Tran-Johnson, E., et al.: Language models (mostly) know what they know. arXiv:2207.05221 (2022)
12. Kossen, J., Han, J., Razzak, M., Schut, L., Malik, S., Gal, Y.: Semantic entropy probes: Robust and cheap hallucination detection in LLMs. arXiv:2406.15927 (2024)
13. Leng, S., Zhang, H., Chen, G., Li, X., Lu, S., Miao, C., Bing, L.: Mitigating object hallucinations in large vision-language models through visual contrastive decoding. In: CVPR (2024)

14. Manevich, A., Tsarfaty, R.: Mitigating hallucinations in large vision-language models via language-contrastive decoding. In: *ACL Findings*. pp. 6008–6022 (2024)
15. Lau, J.J., Gayen, S., Ben Abacha, A., Demner-Fushman, D.: A dataset of clinically generated visual questions and answers about radiology images. *Scientific Data* **5**(1), 1–10 (2018)
16. Li, C., Wong, C., Zhang, S., Usuyama, N., Liu, H., Yang, J., Naumann, T., Poon, H., Gao, J.: LLaVA-Med: Training a large language-and-vision assistant for biomedicine in one day. *NeurIPS* **36** (2024)
17. Li, Q., Geng, J., Lyu, C., Zhu, D., Panov, M., Karray, F.: Reference-free hallucination detection for large vision-language models. In: *EMNLP*. pp. 4542–4551 (2024)
18. Liao, Z., Hu, S., Zou, K., Fu, H., Zhen, L., Xia, Y.: Vision-amplified semantic entropy for hallucination detection in medical visual question answering. In: *MICCAI* (2025)
19. Liu, B., Zhan, L.M., Xu, L., Ma, L., Yang, Y., Wu, X.M.: SLAKE: A semantically-labeled knowledge-enhanced dataset for medical visual question answering. In: *ISBI*. pp. 1650–1654 (2021)
20. Liu, B., Zou, K., Zhan, L., Lu, Z., Dong, X., Chen, Y., Xie, C., Cao, J., Wu, X.M., Fu, H.: GEMeX: A large-scale, groundable, and explainable medical VQA benchmark for chest X-ray diagnosis. *arXiv:2411.16778* (2024)
21. Liu, H., Xue, W., Chen, Y., Chen, D., Zhao, X., Wang, K., Hou, L., Li, R., Peng, W.: A survey on hallucination in large vision-language models. *arXiv:2402.00253* (2024)
22. Min, S., Krishna, K., Lyu, X., Lewis, M., Yih, W.t., Koh, P., Iyyer, M., Zettlemoyer, L., Hajishirzi, H.: FActScore: Fine-grained atomic evaluation of factual precision in long form text generation. In: *EMNLP*. pp. 12076–12100 (2023)
23. Ostmeier, S., Xu, J., Chen, Z., Varma, M., Blankemeier, L., Bluethgen, C., Michalson, A.E., Moseley, M., Langlotz, C., Chaudhari, A.S., et al.: GREEN: Generative radiology report evaluation and error notation. *arXiv:2405.03595* (2024)
24. Saab, K., Tu, T., Weng, W.H., Tanno, R., Stutz, D., Wulczyn, E., Zhang, F., Strother, T., Park, C., et al.: Capabilities of Gemini models in medicine. *arXiv:2404.18416* (2024)
25. Sellergren, A., Kazemzadeh, S., Jaroensri, T., Kiraly, A., Traverse, M., Kohlberger, T., Xu, S., Jamil, F., Hughes, C., Lau, C., et al.: MedGemma technical report. *arXiv:2507.05201* (2025)
26. Sambara, S., Zhang, S., Banerjee, O., Acosta, J., Fahrner, J., Rajpurkar, P.: Rad-Flag: A black-box hallucination detection method for medical vision language models. *arXiv:2411.00299* (2024)
27. Wang, X., Pan, J., Ding, L., Biemann, C.: Mitigating hallucinations in large vision-language models with instruction contrastive decoding. In: *ACL*. pp. 15840–15853 (2024)
28. Xiao, H., Zhou, F., Liu, X., Liu, T., Li, Z., Liu, X., Huang, X.: A comprehensive survey of large language models and multimodal large language models in medicine. *arXiv:2405.08603* (2024)
29. Yin, S., Fu, C., Zhao, S., Xu, T., Wang, H., Sui, D., Shen, Y., Li, K., Sun, X., Chen, E.: Woodpecker: Hallucination correction for multimodal large language models. *Science China Inf. Sci.* **67**(12), 220105 (2024)
30. Yu, Q., Li, J., Wei, L., Pang, L., Ye, W., Qin, B., Tang, S., Tian, Q., Zhuang, Y.: HalluciDoctor: Mitigating hallucinatory toxicity in visual instruction data. In: *CVPR*. pp. 12944–12953 (2024)

31. Zhang, R., Zhang, H., Zheng, Z.: VL-Uncertainty: Detecting hallucination in large vision-language model via uncertainty estimation. arXiv:2411.11919 (2024)